Bull Earthquake Eng (2016) 14:3175–3194
DOI 10.1007/s10518-016-9943-2

ORIGINAL RESEARCH PAPER

Seismic performance evaluation of traditional timber *Hımış* frames: capacity spectrum method based assessment

Yasemin Didem Aktaş[1,2] · Ahmet Türer[3]

Received: 4 January 2016 / Accepted: 21 May 2016 / Published online: 2 June 2016

Abstract Timber constructions have been widely suggested to be seismically resistant based on post-disaster reconnaissance studies. This observation has, however, remained to a large extent anecdotal due to the lack of experimental work supporting it, especially for certain timber architectural forms, including traditional timber frame "*hımış*" structures. To fill this gap, the authors carried out an extensive full-scale testing scheme using frames of various geometrical configurations, tested under reverse-cyclic lateral loading with/without infill (brick and adobe) or cladding (*bağdadi* and *şamdolma*) (Aktas et al. in Earthq Spectra 30(4):1711–1732, 2014a, b). The tests concluded that *hımış* frames had high energy dissipation capabilities due mostly to nailed connections. Infill/cladding significantly helped improve stiffness and lateral load strength of the frames, and timber type did not seem to make a remarkable impact on the overall behaviour. The current paper, on the other hand, uses test data to calculate capacity/demand ratios based on capacity spectrum method and Eurocode 8 to elaborate more on the performance of "*hımış*" structures under seismic loading. The obtained results are discussed to draw important conclusions with regards to how frame geometry and infill/cladding techniques affect the overall performance.

Keywords Timber frame · *hımış* · Capacity spectrum method

✉ Yasemin Didem Aktaş
y.aktas@ucl.ac.uk

[1] Restoration Program, Middle East Technical University (METU), Dumlupınar Bulvarı, 06800 Çankaya, Ankara, Turkey

[2] Present Address: Epicentre Research Group, Civil, Environmental and Geomatic Engineering, University College London (UCL), Gower Street, London WC1E 6BT, UK

[3] Civil Engineering Department, Middle East Technical University (METU), Dumlupınar Bulvarı, 06800 Çankaya, Ankara, Turkey

1 Introduction

Traditional *hımış* houses are composite structures, characterized by upper floors composed of a timber frame load-bearing system constructed on top of a masonry ground floor that may or may not be timber-strengthened. Despite slight differences in different regions, especially in terms of infill/cladding materials/types, the same form and design principles were generally applied over a vast geographic area, regardless of differences in climate, extending from the inner sections of Anatolia to the Balkans and Greece (Kuban 1995; Cerasi 1998; Sözen 2001).

There are many post-disaster studies reporting a favourable seismic performance of timber frame "*hımış*" houses (e.g. see Ambraseys et al. 1968 for 1967 Mudurnu Earthquake; Sahin Güçhan 2007; Penzien and Hanson 1970 for 1970 Gediz Earthquake; Erdik et al. 1992 for 1992 Erzincan Earthquake; Gülhan and Özyörük Güney 2000; Tobriner 2000, and Langenbach 2007 for 1999 Düzce Earthquake; Demirtaş et al. 2000 for 2000 Orta Earthquake). In those cases where "*hımış*" houses were reported to have behaved poorly, the damage was often either triggered by the failure of masonry ground floor or initiated by non-structural masonry elements such as chimneys, or associated with lack of maintenance, material degradation, improper connections, and heavy roofs (e.g. see Erdik et al. 2002a, b; Koçyiğit et al. 2002 for 2002 Çay Earthquake and Erdik et al. 2003 for 2003 Bingöl Earthquake).

Despite these post-disaster observations, the seismic resistance of "*hımış*" houses has remained largely anecdotal due to the lack of experimental work supporting this conclusion. To provide this empirical baseline data, in 2010 a research project was set up and funded by the Scientific and Technological Research Council of Turkey (106M499). To this end, a number of frame tests and capacity/demand calculations were carried out with the aim of assessing and quantifying the seismic resistance of traditional timber *hımış* frames. The findings from these frame tests have been presented and discussed elsewhere (Aktas et al. 2014a, b). This paper reports the ATC-40 based capacity calculations using the data obtained from the frame tests and comparison of these against demand values

Fig. 1 An overall view of the test setup

calculated by using Eurocode 8 (2004), in order to evaluate the seismic performance of each frame with different geometrical configurations, with and without infill/cladding.

2 Frame tests

For frame tests, a total of 6 frames that reflect the geometrical and constructive features of traditional *hımış* frames were selected from Safranbolu, a UNESCO World Heritage site in northern Turkey for its authentic townscape characterized by *hımış* houses (for more detailed information about frame selection, see Aktas et al. 2014a). Out of 6 selected frame geometries, 2 were built twice by local builders using yellow pine and fir (see Aktas et al. 2014a for material properties), to investigate not only the effect of geometrical configuration but also the type of timber on the structural behaviour. Therefore, a total of 8 full-scale frames were tested under reverse cyclic lateral loading in with and without-infill/cladding states to investigate the contribution of infill/cladding to the structural response (Fig. 1).

2 infill (adobe and brick) and 2 cladding (*şamdolma* and *bağdadi*) techniques were used for a total of 8 test frames (for details of infill and cladding techniques see Aktas et al. 2014a). The details of frames and infill combinations are given in Table 1. Adobe blocks as well as all mortar and plaster were prepared so as to reflect local traditional practices (Aktas et al. 2014a, b). Solid bricks to use for brickwork infill were sourced from demolished historic buildings from the late nineteenth century. All frames were built and repaired by local builders who are experienced on the construction of new timber frame houses and on the restoration of existing ones. Only nails were used in the construction of the frames at the connections in line with traditional practices. Each frame was first tested without infill or cladding. The frames were intentionally not severely damaged at this stage in order to be able to retest them later with infill or cladding (in addition, laboratory safety regulations also prevented testing some of the highly flexible bare frames until or beyond ultimate strength level to identify descending portion of the load–deflection curve). The bare frames were repaired after initial testing, by using the same number and type of nails (12 cm long 4.5 mm thick) at the connections where damage was concentrated and reused for tests with infill/cladding. Frames were plastered after infill/cladding and restested under reverse-cyclic loading. Please note that also in this stage some of the frames were not pushed to their capacity for safety reasons (beyond a certain drift level the falling of plaster or infill material posed risk for measurement instruments and technicians). The envelope curves for lateral load versus lateral displacement relationships of the tested frames for with and without infill/cladding states are given in Fig. 2 and Table 1. The P-Δ effect of the deformed frames was neglected since only about maximum of 7 % of the distributed load on the frame was outside the base area on the ground.

The results obtained at this stage of the study can be summarized as follows (Aktas et al. 2014a, b): (1) type of timber (yellow pine or fir) does not seem to be important in the test set examined here as failures always occur at the nailed connections and wood is not stressed to its strength limits. Because of the damage mechanism at the nailed connections, based on partial in and out movement of the nails, the observed failures occur in a highly ductile way; (2) infill/cladding increases the lateral load strength of a timber frame, however the increase in the lateral load strength is nearly always less than weight increase due to infill/cladding; (3) among all the infill and cladding techniques, *bağdadi* seems to be the one that provides the best improvement in frame's behaviour, since it seems to satisfy

Table 1 Tested frames

Frame		Infill/cladding	General information	Resulting lateral displacement (mm) lateral load (kN) graphs (in the same scale)
1		Adobe Masonry 	(H × W): 325 × 310 cm Yellow Pine 2 windows: 135 × 67 cm each Opening area/total area: 0.18 Opening width/net width (OtN): 0.76	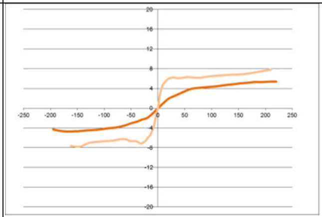
2		Adobe Masonry 	(H × W): 360 × 330 cm Yellow Pine No windows Opening area/total area: 0 Opening width/net width (OtN): 0	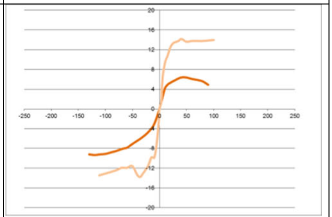
3		*Şamdolma* 	(H × W): 360 × 330 cm Fir No windows Opening area/total area: 0 Opening width/net width (OtN): 0	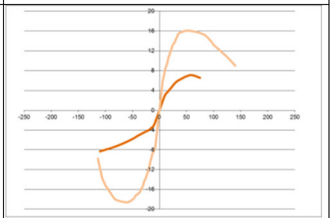
4		Brick Masonry 	(H × W): 325 × 310 cm Fir 2 windows: 135 × 67 cm each Opening area/total area: 0.18 Opening width/net width (OtN): 0.76	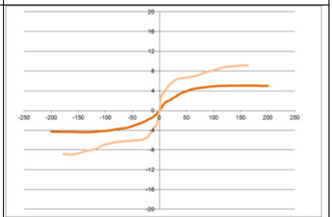

Table 1 continued

5		*Bağdadi* 	(H × W): 330 × 370 cm Yellow Pine 3 windows: 116 × 62 cm each Opening area/total area: 0.18 Opening width/net width (OtN): 1.01	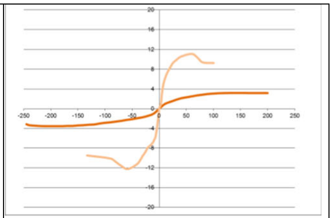
6	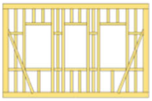	*Şamdolma* 	(H × W): 340 × 520 cm Yellow Pine 3 windows: 157 × 93 cm each Opening area/total area: 0.25 Opening width/net width (OtN): 1.16	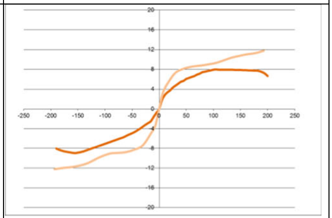
7	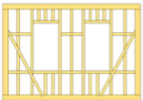	Brick Masonry 	(H × W): 340 × 485 cm Yellow Pine 2 windows: 169 × 89.5 cm each Opening area/total area: 0.18 Opening width/net width (OtN): 0.58	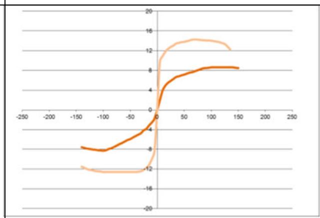
8	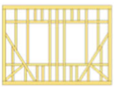	*Bağdadi* 	(H × W): 300 × 400 cm Yellow Pine 2 windows: 156 × 75 cm each Opening area/total area: 0.19 Opening width/net width (OtN): 0.60	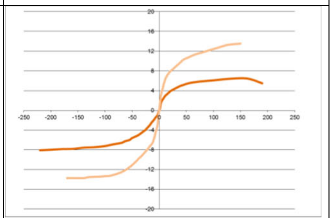

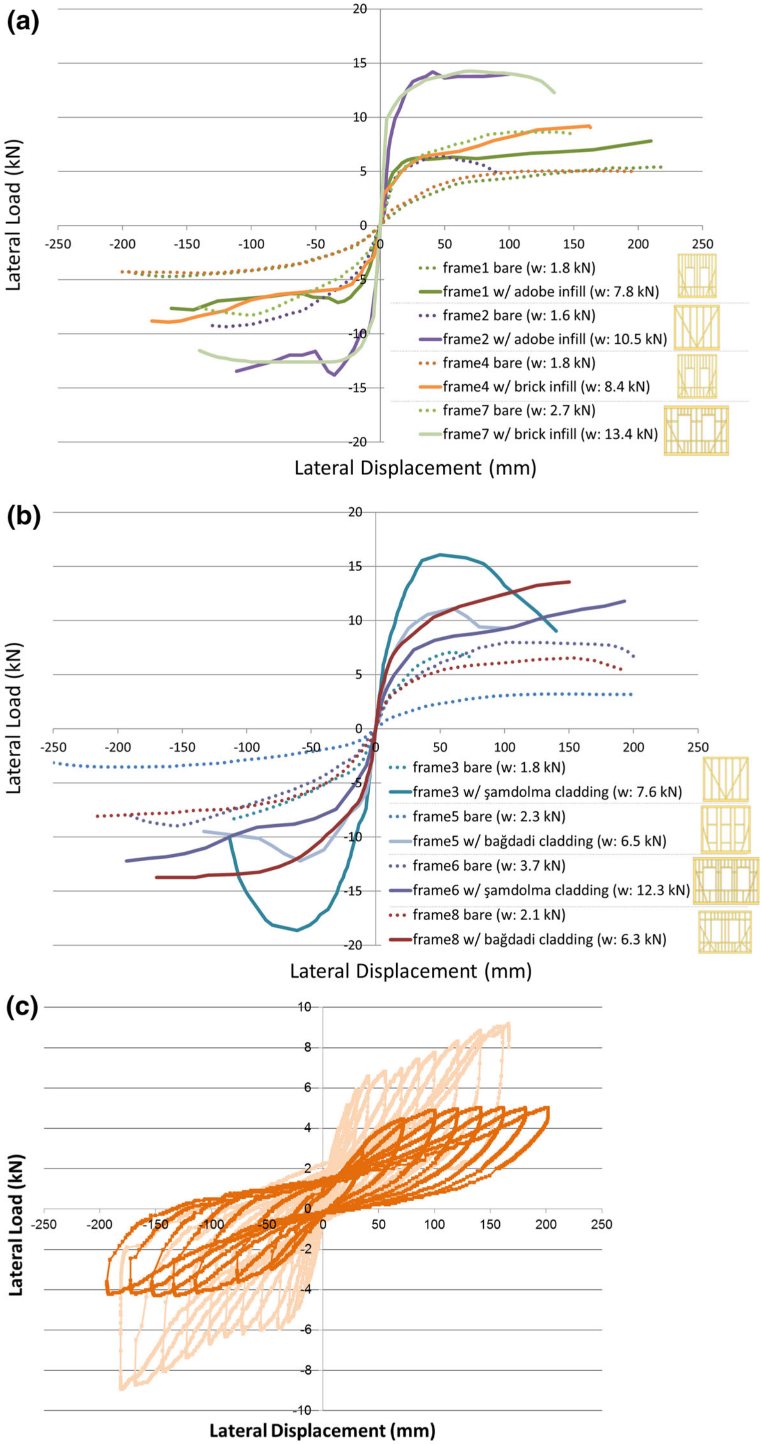
(a)
Lateral Load (kN)
Lateral Displacement (mm)
frame1 bare (w: 1.8 kN)
frame1 w/ adobe infill (w: 7.8 kN)
frame2 bare (w: 1.6 kN)
frame2 w/ adobe infill (w: 10.5 kN)
frame4 bare (w: 1.8 kN)
frame4 w/ brick infill (w: 8.4 kN)
frame7 bare (w: 2.7 kN)
frame7 w/ brick infill (w: 13.4 kN)
(b)
Lateral Load (kN)
Lateral Displacement (mm)
frame3 bare (w: 1.8 kN)
frame3 w/ şamdolma cladding (w: 7.6 kN)
frame5 bare (w: 2.3 kN)
frame5 w/ bağdadi cladding (w: 6.5 kN)
frame6 bare (w: 3.7 kN)
frame6 w/ şamdolma cladding (w: 12.3 kN)
frame8 bare (w: 2.1 kN)
frame8 w/ bağdadi cladding (w: 6.3 kN)
(c)
Lateral Load (kN)
Lateral Displacement (mm)

◀**Fig. 2** Envelope curves of lateral displacement-lateral load relationships for frames **a** before and after infill and **b** before and after cladding (w stands for weight), and **c** an example to full lateral displacement-lateral load curves, obtained for Frame#4 without and with brick infill

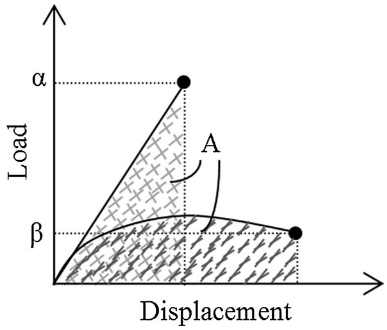

Fig. 3 Energy-based definition of seismic reduction "behaviour" factor, R (R = α/β)

the optimum combination of a high increase in lateral load strength and a low increase in weight; and (4) the frame behaviour is highly dependent on workmanship, which was observed to be highly scattered even in a limited set of frames built by the same group of builders as here. Especially the connection quality (number of nails at each connection and their driving angles) varied from frame to frame and within the same frame, which influenced the strength and stiffness. This, among other factors, makes it hard to generalize the findings.

In addition, based on the obtained lateral load-lateral displacement curves, "energy based" reduction factors were calculated. For this aim, the area underneath the load–deflection curve was calculated and set equal to the area underneath the linear load–deflection graph obtained by extending the initial slope of the load–deflection graph (Fig. 3). The ratio of the base shears corresponding to the ultimate points for the linear and nonlinear curves was taken as energy based reduction factor (R). The R values for the without and with infill/cladding cases were found to be equal to 2.96 ($\sigma_{dev} = 1.05$) and 3.72 ($\sigma_{dev} = 1.18$), respectively, which are quite comparable to the values reported in the relevant codes.

3 Capacity spectrum method based assessment

In this study, the seismic capacity of timber frames was evaluated by using the capacity spectrum method (CSM). CSM was developed in the 1970's, and especially from the introduction of ATC 40 (1996) onwards has been widely integrated in common guidance documents as a nonlinear static analysis method for a rapid structural evaluation of existing and new buildings. This method involves coordinate transformation from physical axes of displacement to period and spectral acceleration coordinates, and provides a clear, graphical representation of how a building is expected to behave under a certain seismic event (Freeman 1998). In the past, the CSM based evaluation of timber frame structures was discussed and made on analytical models (e.g. Kawai 1999, 2000; Hayashi et al. 2008). In this study, CSM has been applied following the ATC-40 procedures.

The constants regarding modal mass coefficient (α_1) and modal participation factor (PF_1) for the first natural mode of the tested timber test frames, which can be represented as a single degree-of-freedom system, were taken as 0.8 and 1.4, respectively, as described in ATC-40 (1996). Structural behaviour type, which is a function of the structure condition and shaking duration, also needs to be defined for the ATC-40 based implementation of CSM. The structure condition is defined as a function of having reliable hysteretic behaviour and age of the structure. Although the hysteretic response of the tested frames seem to be acceptably good (Fig. 2), because in this case the tested timber frame behaviour is based on a number of uncontrolled, inconsistent, and not standardized parameters (e.g. number of nails, driving angles of nails, workmanship), structural behaviour type was selected as Type C, which is defined as 'poor existing building' or "average existing building under long shaking duration" (ATC 1996). The closest alternative, Type B, was ruled out since it corresponds to "average existing building" with short shaking duration or "essentially new building" with long shaking duration and is not compatible with the timber frames considered in this study. Although damping ratios for Type C are relatively

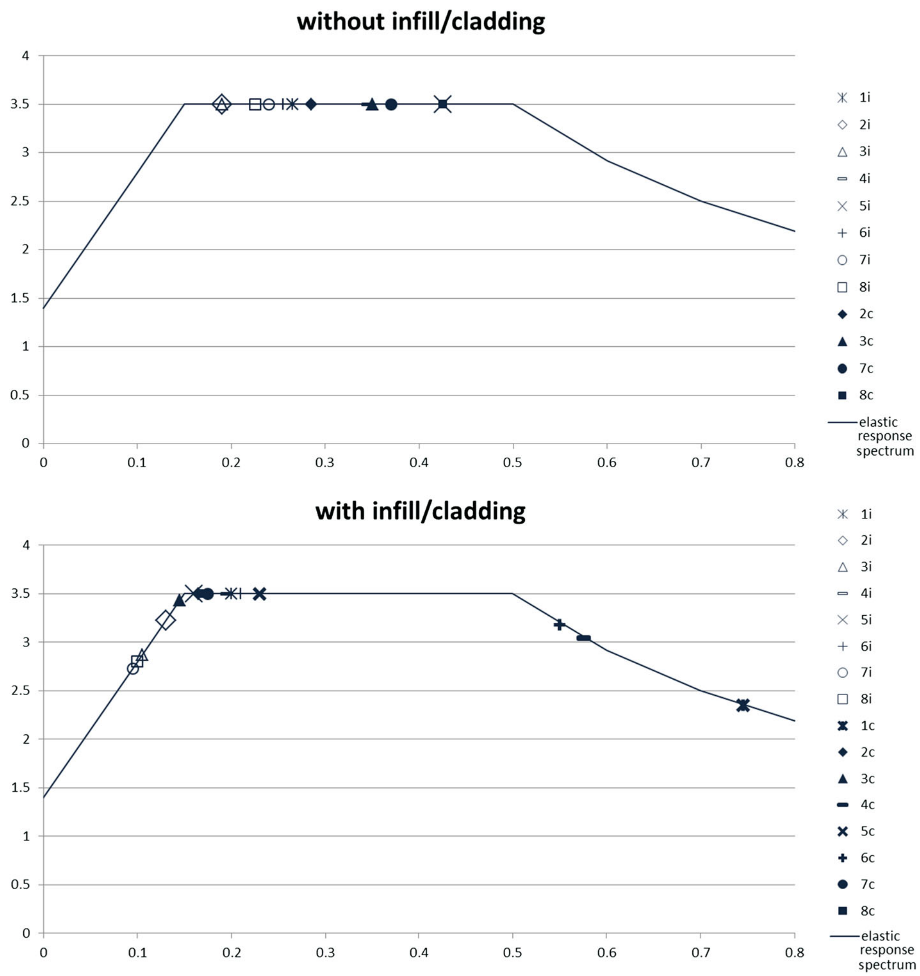

Fig. 4 Period values obtained from ATC-40 capacity calculations shown on 5 % elastic response spectrum drawn according to EC8

low compared to other types and the tested frames exhibit larger damping ratios, Type C was selected anyways to be on the safe side due to above-mentioned unreliability/uncertainty conditions associated with the tested timber frames.

The reduced response spectrums (modified for damping ratios different than 5 %) were drawn by using the spectral reduction factors, SR_A and SR_V, which are calculated in accordance with ATC-40 1996, and checked against defined minimum values, as well as the seismic coefficients, C_A and C_V. The C_A and C_V values are functions of (a) seismic zone factor (taken as 4, which is the worst case in a scale out of 4) (b) soil profile type (taken as E, which is the softest soil case in a scale from A to E) and (c) ZEN factors, which is calculated by multiplying the seismic zone factor Z (taken as 0.4 for as suggested for Zone 4 sites), earthquake hazard level factor E (taken as 1.25 as suggested for Zone 4 sites) for maximum earthquake and near source factor N (taken as 1.0 as suggested, assuming the closest distance to known seismic source is larger than 15 km distance). All these parameters are independent of structure type by definition. According to the described procedure, first, the capacity curves were obtained by using the Eqs. 1 and 2.

$$S_a = \frac{V/W}{\alpha_1} \tag{1}$$

and

$$S_d = \frac{\Delta_{roof}}{PF_1 \varphi_{roof,1}} \tag{2}$$

where, S_a and S_d are spectral acceleration and spectral displacement, V is the base shear, W is building dead weight plus likely live loads, α_1 is the modal mass coefficient for the first natural mode, Δ_{roof} is top displacement, PF_1 is the modal participation factor for the first natural mode, and $\varphi_{roof,1}$ is amplitude of mode 1 at the roof level.

The period values obtained from the capacity calculations shown on the 5 % elastic response spectrum are given in Fig. 4. Here the effect of change in damping ratios was not taken into consideration since the aim of this comparison is simply to see how structural period T changes from T_i (period in the linear range) to T_a (period at the

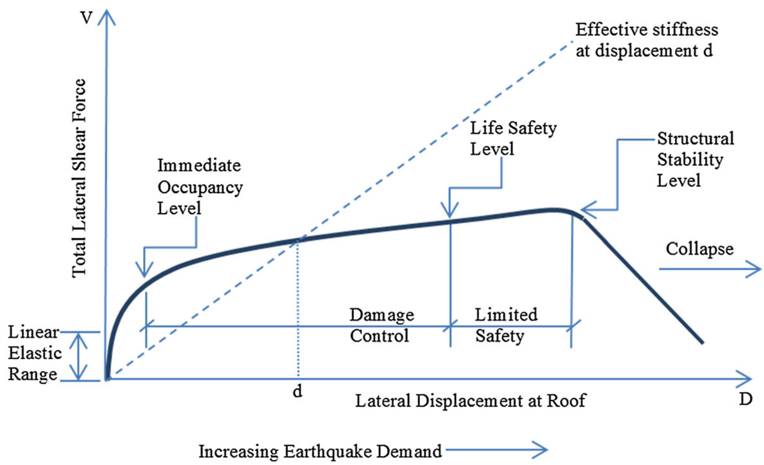

Fig. 5 Typical capacity curve

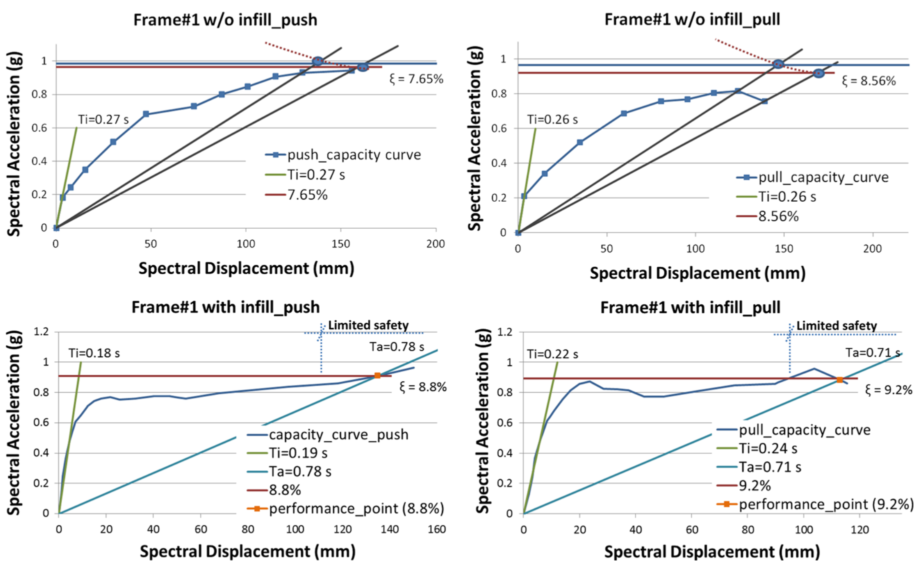

Fig. 6 S_d–S_a graphs of Frame#1 without and with infill, and for push and pull directions, respectively (demand curve for the damping value obtained for the last data point of the capacity curve is given as a reference)

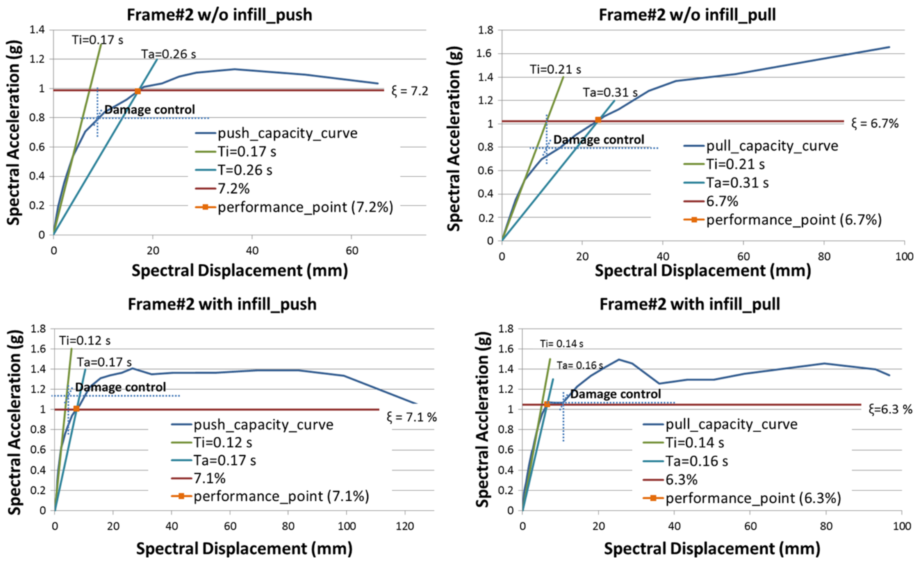

Fig. 7 S_d–S_a graphs of Frame#2 without and with infill, and for push and pull directions, respectively

performance point) on the response spectrum in an ascending or descending manner. Structural performance levels (immediate occupancy, damage control, life safety, limited safety, and structural stability) are generically defined as in Fig. 5. The resulting spectral displacements versus spectral acceleration graphs for each of the frames without and with

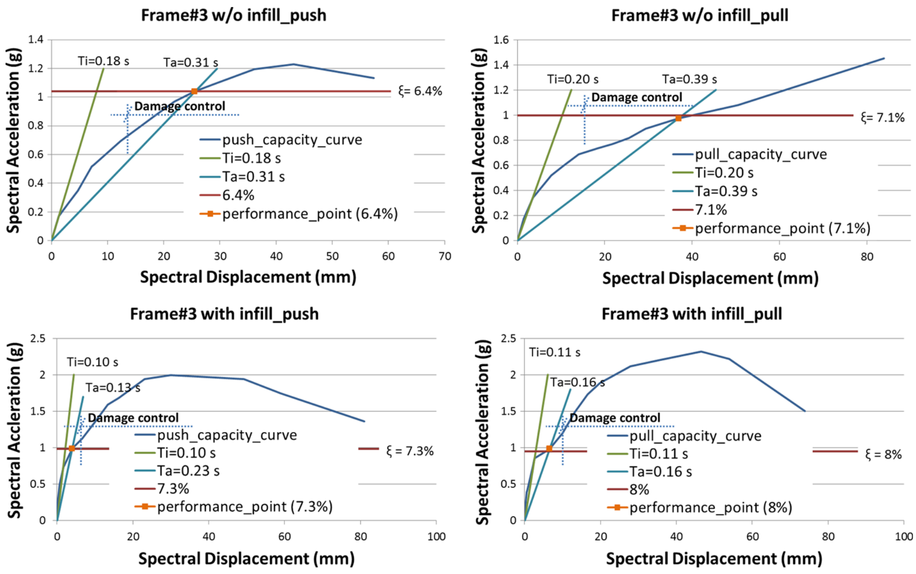

Fig. 8 S_d–S_a graphs of Frame#3 without and with infill, and for push and pull directions, respectively

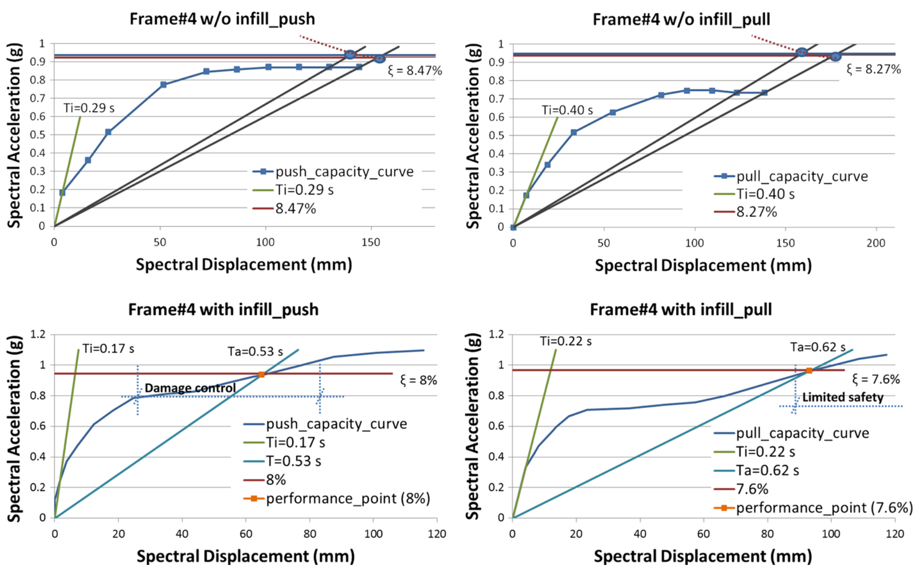

Fig. 9 S_d–S_a graphs of Frame#4 without and with infill, and for push and pull directions, respectively (demand curve for the damping value obtained for the last data point of the capacity curve is given as a reference)

infill/cladding are given in Figs. 6, 7, 8, 9, 10, 11, 12 and 13 with the resulting structural performance levels for each case as defined in ATC-40 (1996). The obtained results are summarized in Table 2.

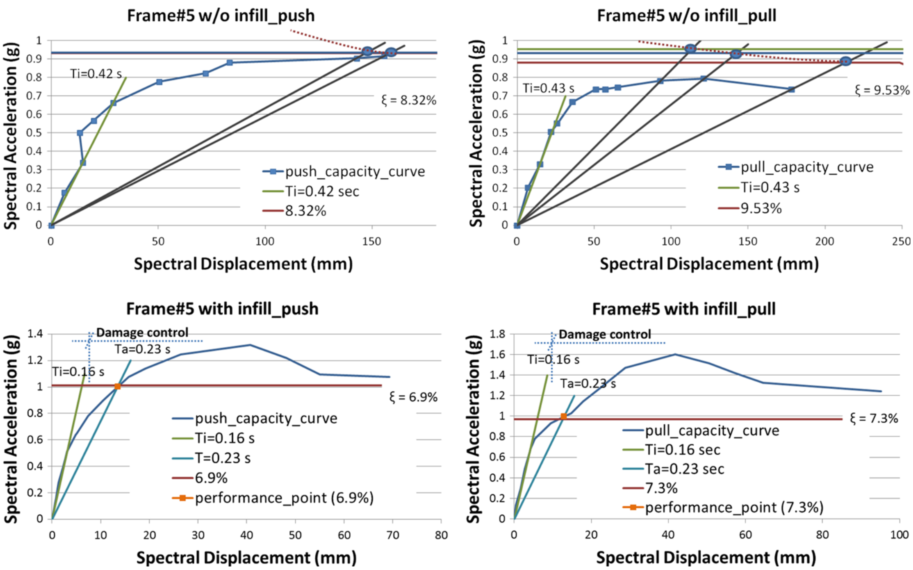

Fig. 10 S_d–S_a graphs of Frame#5 without and with infill, and for push and pull directions, respectively (demand curve for the damping value obtained for the last data point of the capacity curve is given as a reference)

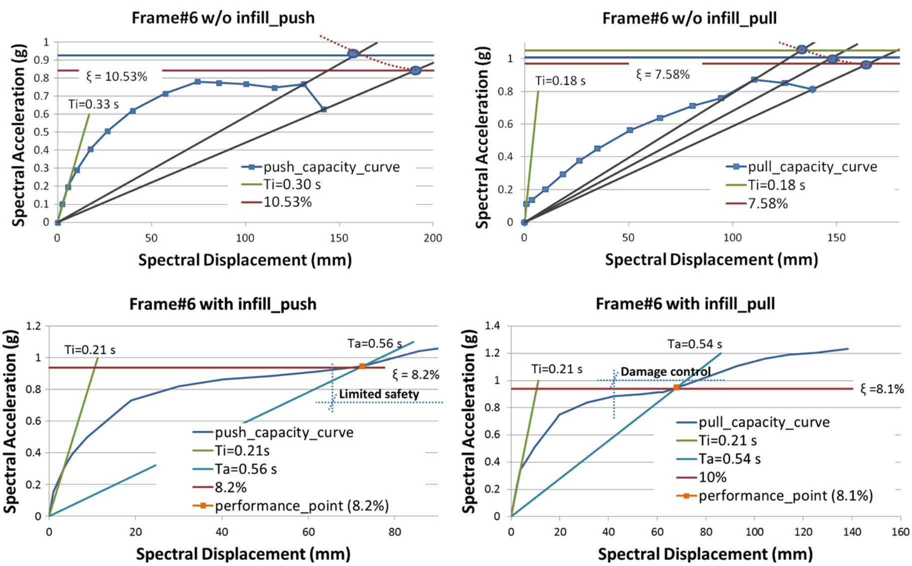

Fig. 11 S_d–S_a graphs of Frame#6 without and with infill, and for push and pull directions, respectively (demand curve for the damping value obtained for the last data point of the capacity curve is given as a reference)

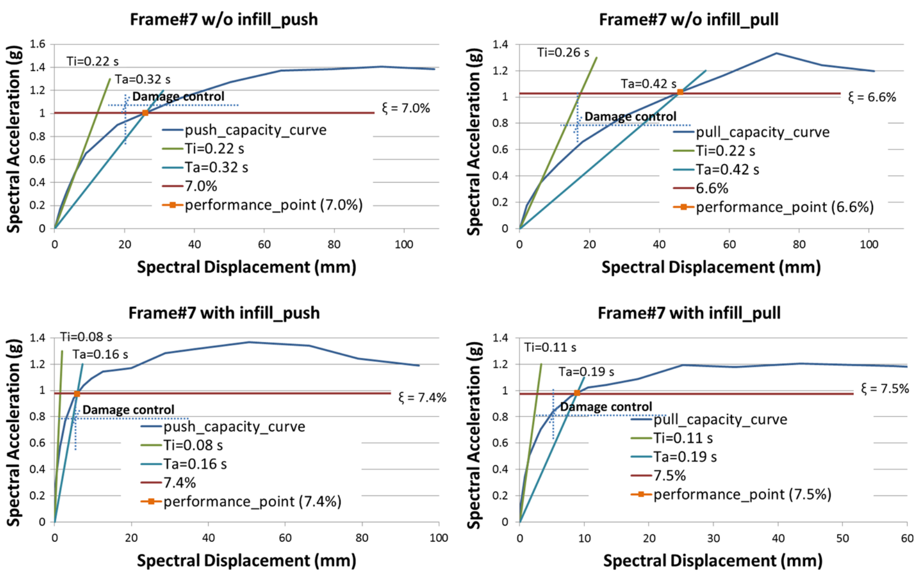

Fig. 12 S_d–S_a graphs of Frame#7 without and with infill, and for push and pull directions, respectively

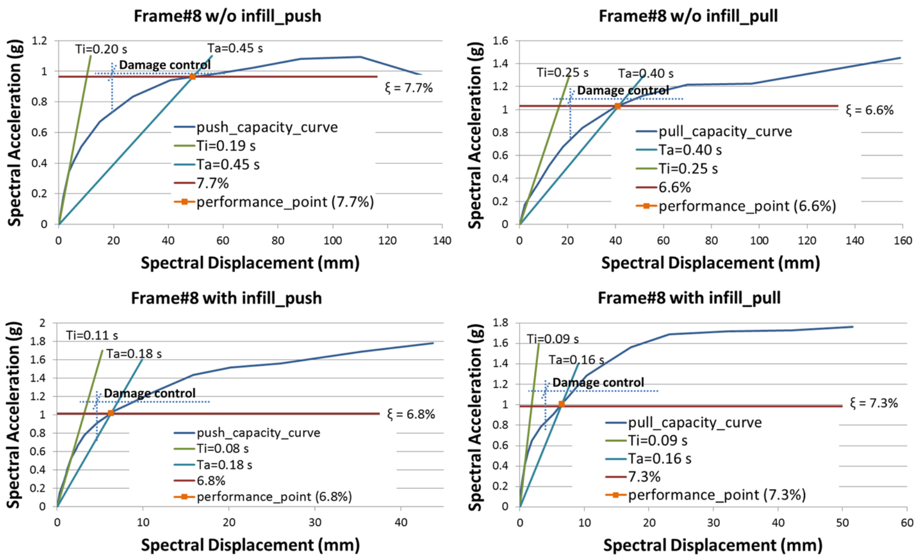

Fig. 13 S_d–S_a graphs of Frame#8 without and with infill, and for push and pull directions, respectively

4 Demand calculations

In order to calculate the behaviour factor (q) for the tested frames, an additional set of demand calculations were carried out based on Eurocode 8 (2004) and used for capacity/demand comparisons.

Table 2 Results of the capacity calculations for each frame without and with infill/cladding

Frame	Without-infill state		With-infill/cladding state	
	Push	Pull	Push	Pull
1	$T_i = 0.27$ s	$T_i = 0.26$ s	$T_i = 0.18$ s; $T_a = 0.78$ s $S_d = 135$ mm; $\xi = 8.8$ %	$T_i = 0.22$ s; $T_a = 0.71$ s $S_d = 113$ mm; $\xi = 9.2$ %
2	$T_i = 0.17$ s; $T_a = 0.26$ s $S_d = 17$ mm; $\xi = 7.2$ %	$T_i = 0.21$ s; $T_a = 0.31$ s $S_d = 24$ mm; $\xi = 6.7$ %	$T_i = 0.12$ s; $T_a = 0.17$ s $S_d = 7.5$ mm; $\xi = 7.1$ %	$T_i = 0.14$ s; $T_a = 0.16$ s $S_d = 6.5$ mm; $\xi = 6.3$ %
3	$T_i = 0.18$ s; $T_a = 0.31$ s $S_d = 25.5$ mm; $\xi = 6.4$ %	$T_i = 0.20$ s; $T_a = 0.39$ s $S_d = 36.9$ mm; $\xi = 7.1$ %	$T_i = 0.10$ s; $T_a = 0.13$ s $S_d = 4$ mm; $\xi = 7.3$ %	$T_i = 0.11$ s; $T_a = 0.16$ s $S_d = 6.6$ mm; $\xi = 8$ %
4	$T_i = 0.29$ s	$T_i = 0.40$ s	$T_i = 0.17$ s; $T_a = 0.53$ s $S_d = 65$ mm; $\xi = 8$ %	$T_i = 0.22$ s; $T_a = 0.62$ s $S_d = 93.2$ mm; $\xi = 7.6$ %
5	$T_i = 0.42$ s	$T_i = 0.43$ s	$T_i = 0.16$ s; $T_a = 0.23$ s $S_d = 13.5$ mm; $\xi = 6.9$ %	$T_i = 0.16$ s; $T_a = 0.23$ s $S_d = 12.9$ mm; $\xi = 7.3$ %
6	$T_i = 0.33$ s	$T_i = 0.18$ s	$T_i = 0.21$ s; $T_a = 0.56$ s $S_d = 72.5$ mm; $\xi = 8.2$ %	$T_i = 0.21$ s; $T_a = 0.54$ s $S_d = 68$ mm; $\xi = 8.1$ %
7	$T_i = 0.22$ s; $T_a = 0.32$ s $S_d = 26$ mm; $\xi = 7.0$ %	$T_i = 0.26$ s; $T_a = 0.42$ s $S_d = 46$ mm; $\xi = 6.6$ %	$T_i = 0.08$ s; $T_a = 0.16$ s $S_d = 5.6$ mm; $\xi = 7.4$ %	$T_i = 0.11$ s; $T_a = 0.19$ s $S_d = 8.9$ mm; $\xi = 7.5$ %
8	$T_i = 0.20$ s; $T_a = 0.45$ s $S_d = 49$ mm; $\xi = 7.7$ %	$T_i = 0.25$ s; $T_a = 0.40$ s $S_d = 41$ mm; $\xi = 6.6$ %	$T_i = 0.11$ s; $T_a = 0.18$ s $S_d = 6.3$ mm; $\xi = 6.8$ %	$T_i = 0.09$ s; $T_a = 0.16$ s $S_d = 6.5$ mm; $\xi = 7.3$ %

$$F_b = S_d(T_1) \times m \times \lambda \tag{3}$$

In Eq. 3 F_b stands for base shear force, i.e. seismic demand, m for the total mass of the building and λ for the correction factor, which was taken equal to 1.0 as suggested by Eurocode 8 (2004) and finally $S_d(T_1)$ for the ordinate of the design spectrum at period T_1 (please note that since all tested frames pass into the nonlinear range during a design earthquake (Figs. 6, 7, 8, 9, 10, 11, 12, 13), S_d coefficients defined in Eurocode 8 were used instead of S_e coefficients).

The base shear demands (F_b) were calculated using the period values (T_a) obtained for those frames whose capacity spectra resulted in a performance point. Then, the behaviour factor (q) was back-calculated for each test case using the equations given in Eurocode 8 for the calculation of the design spectrum. The test frames yielded an average q value of 1.9 ($\sim$2) for without infill/cladding cases and 2.6 for with infill/cladding cases, allowing a

Table 3 Capacity and demand values calculated for each frame without and with infill/cladding in the linear and non-linear states (NPP, NA, L, NL, and *şd* stand for no performance point, not applicable, linear, non-linear and *şamdolma* respectively)

Frame #	OtN		Without infill/cladding								With infill/cladding								
			Load bearing capacity (kN)		T_i (s)	T_a (s)	Demand Fb (kN)		Capacity/demand		Infill/cladding	Load bearing capacity (kN)		T_i (s)	T_a (s)	Demand Fb (kN)		Capacity/demand	
			L	NL			L	NL	L	NL		L	NL			L	NL	L	NL
2	0	Push	3.03	6.38	0.17	0.26	10.57	5.56	0.29	1.15	adobe	6.93	14.18	0.12	0.17	16.97	9.04	0.41	1.57
	0	Pull	2.92	>9.36	0.21	0.31	10.57	5.56	0.28	>1.68		7.24	13.80	0.14	0.16	16.97	9.04	0.43	1.53
3	0	Push	0.98	7.07	0.18	0.31	10.92	5.75	0.09	1.23	*şd*	5.90	16.03	0.1	0.13	13.91	7.10	0.42	2.26
	0	Pull	1.97	>8.33	0.2	0.39	10.92	5.75	0.18	>1.45		6.89	18.66	0.11	0.16	13.91	7.41	0.50	2.52
7	0.58	Push	2.96	8.57	0.22	0.32	12.17	6.40	0.24	1.34	brick	3.92	14.18	0.08	0.16	19.88	10.59	0.20	1.34
	0.58	Pull	2.10	8.13	0.26	0.42	12.17	6.40	0.17	1.27		4.43	12.50	0.11	0.19	19.88	10.59	0.22	1.18
8	0.60	Push	2.00	6.38	0.2	0.45	11.27	5.93	0.18	1.08		3.99	>13.43	0.11	0.18	12.66	6.74	0.31	>1.99
	0.60	Pull	1.01	>8.47	0.25	0.4	11.27	5.93	0.09	>1.43	*bağdadi*	3.13	>13.33	0.09	0.16	12.66	6.74	0.25	>1.98
1	0.76	Push	1.05	>5.42	0.27	NPP	10.96	NA	0.10	NA	adobe	3.92	>7.82	0.18	0.78	7.52	7.52	0.52	>1.04
	0.76	Pull	1.21	4.7	0.26	NPP	10.96	NA	0.11	NA		3.95	>8.81	0.22	0.71	7.52	7.52	0.53	>1.17
4	0.76	Push	1.05	>5.01	0.29	NPP	10.96	NA	0.10	NA	brick	2.00	>9.19	0.17	0.53	7.87	7.87	0.25	>1.17
	0.76	Pull	1.01	>4.30	0.4	NPP	10.96	NA	0.09	NA		2.79	>8.95	0.22	0.62	7.87	7.87	0.35	>1.14
5	1.01	Push	2.00	3.17	0.42	NPP	11.55	NA	0.17	NA	*bağdadi*	4.95	11.10	0.16	0.23	6.84	6.84	0.72	1.62
	1.01	Pull	1.97	>3.47	0.43	NPP	11.55	NA	0.17	NA		5.18	12.23	0.16	0.23	6.84	6.84	0.76	1.79
6	1.16	Push	2.00	7.96	0.33	NPP	13.61	NA	0.15	NA	*şd*	3.03	11.79	0.21	0.56	9.99	9.99	0.30	1.18
	1.16	Pull	1.15	8.88	0.18	NPP	13.61	NA	0.08	NA		3.40	12.23	0.21	0.54	9.99	9.99	0.34	1.22

Listed from smallest to largest OtN value categorization of "Medium capacity to dissipate energy—DCM" according to Table 8.1 in EC8. Although an initial guess of 3 was expected for the test frames because of the highly ductile nailed connections, test results yielded slightly lower q values, which was attributed to the fact that the infill (brick or adobe) and cladding (strips of wood panels connected with single nail at each point generating a mechanism during lateral deformation) had minor diaphragm action.

The results obtained from frame tests and calculated capacity points were further used to calculate linear and non-linear capacity to demand ratios, which can be seen in Table 3. The linear range capacity to demand ratios remained below 1.0 for all frames indicating they pass into the nonlinear range.

5 Discussion

In this study the capacity curves and performance points were obtained for each test by using ATC-40 procedures. Then, the ultimate capacity obtained for each frame was compared against the demand values calculated using Eurocode 8. The results indicate that a performance point cannot be obtained for the frames #1, 4, 5, and 6 when they are tested in *without infill/cladding state*; therefore, they collapse under the maximum earthquake defined by ATC-40. These four frames have large window openings and are relatively short in length, while frames #2 and 3 do not have window openings and #7 and 8 have smaller window to length ratio. A number of geometrical features were evaluated to see if there was a systematic correlation with the structural parameters, and the ratio of "total width of the openings (windows, doors etc.)" to "net width (total width minus the width of the openings") (henceforward OtN ratio) has been found meaningful for a quick evaluation of the performance of the bare frame set tested here. The lateral displacement-lateral load curves obtained for bare frames with OtN ratio less than 2/3 result in a performance point and therefore based on this study these frames can be said to survive a maximum earthquake (Fig. 14; Table 1).

Comparison of the frames with infill or cladding also reveals interesting results in terms of spectral displacement (S_d) values obtained for performance points. Geometric properties discussed in the previous paragraph showed OtN ratio made some frames more vulnerable against seismic action. The frames with good geometrical properties, i.e., OtN $< 2/3$, still

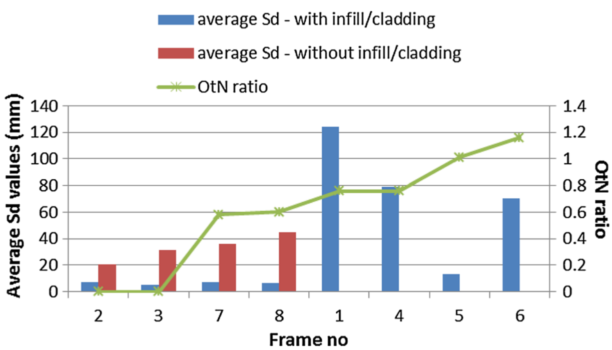

Fig. 14 Comparison of frames in terms of spectral displacement and OtN values

had superior performance regardless of their infill material or cladding technique (Fig. 14). Besides, frames with geometrical disadvantages, i.e., OtN > 2/3, may have improved performance if *bağdadi* cladding technique is used. *Bağdadi* cladding is composed of thin laths (about 10 mm thick, 20–30 mm wide) being the lightest technique among all infill/cladding methods. Therefore, the major benefit of *bağdadi* comes from its relatively denser and continuous bracing effect. Although frames #5 and 6 have similar OtN values (1.01 and 1.16, respectively), the spectral displacement (S_d) values obtained for them are approximately 13 mm (immediate occupancy) and 70 mm (life safety), respectively. *Bağdadi* cladding used in the frame #5 was shown to be superior to *şamdolma* (about 10 mm thick, 70–100 mm wide, and relatively long timber laths), which was the cladding technique used for frame #6. Although differences in the geometrical configuration must have also played a role in the obtained results, the number of nails used in unit area is about 5–6 times more in *bağdadi* than *şamdolma* generating a relatively better diaphragm action between the timber frame members (Fig. 14).

Brick infill can be compared against timber cladding (*bağdadi* and *şamdolma*), examining results of frames #4 and 5 as well as #7 and 8. Although the OtN value of frame #5 (1.01) is larger than that of frame #4 (0.76), the S_d values for frame #5 with *bağdadi* cladding and frame #4 with brick infill are about 13 mm (immediate occupancy, Fig. 10) and 79 mm (life safety Fig. 9), respectively. This result shows that *bağdadi* cladding can outperform the brick infill making a disadvantaged bare frame perform better when cladded.

Behaviour factors (q) were calculated for each one of the tested frames with a performance point using equations given in Eurocode 8. The q values for without and with infill/cladding test results were on average found to be 1.9 and 2.6, considered as "Medium capacity to dissipate energy—DCM" design concept and ductility class.

The calculated capacity to demand ratios for linear and non-linear ranges (Table 3) resulted values below 1.0 for all frames in the linear range, indicating that they pass into the nonlinear range. The capacity to demand ratios may be considered as a factor of safety and values smaller than 1.0 would mean the structure will fail in the corresponding range. Similarly, the factor of safety values obtained for the frames with OtN ratios higher than 2/3 appear to be only in the range of 1, even with infill/cladding (Table 3). The average ratios for the nonlinear range is 1.54 for all test frames, while frames with adobe/brick infill and frames with cladding had average values of 1.27 and 1.82, respectively. The capacity to demand ratio average for bare frames in the nonlinear range was found to be 1.33 which is reduced to 1.27 if infill is used and increased to 1.82 if cladding is used. Please note that the capacity and hence the capacity to demand ratios reported for frames that could not be pushed to their limits were expressed as greater than (>) the calculated value.

Additionally, while interpreting the obtained results it should be not be forgotten that if a 3D "box" with frames at four sides was tested, higher load bearing capacities would be reached as the perpendicular walls would provide additional uplift resistance.

6 Conclusions

The major conclusions drawn from this study are as follows:

- All timber frames with infill/cladding yielded a performance point regardless of the infill material or cladding technique, which means they will survive a design earthquake.

- Although the strength and spectral displacement values obtained for each tested frame are quite scattered, this diversity in the results can to a large extent be explained based on infill/cladding type and the "window length" to "net frame length" (total length minus window lengths) ratio (OtN). For instance, the OtN was found to be a good indicator for rapid geometric evaluation of bare frames (without infill or cladding): bare frames with OtN ratio being smaller than 2/3 have resulted in performance points while others collapsed under design earthquake loading. Similarly, frames with OtN higher than 2/3 have relatively low factors of safety even with infill/cladding especially since infill often times generates additional inertial mass, which increases seismic demand. Additionally, *bağdadi* type cladding was shown to be superior to other infill (brick, adobe) and cladding (*şamdolma*) types. Furthermore, *bağdadi* was shown to alter the poor performance of bare frames with OtN value larger than 2/3 (e.g. frame #5).
- All performance points converged on the capacity curves were found in the nonlinear range; therefore, all frames with infill/cladding are incapable of bearing seismic demand in the linear range and they pass into nonlinear state. Therefore, frames do not remain elastic and exhibit certain amount of damage, as expected.
- The nonlinear behaviour of frames was also supported by the capacity to demand ratios, which were smaller than 1.0 for the linear range and greater than 1.0 for the nonlinear range. The cladded frames yielded larger capacity to demand ratio averages in the nonlinear range (1.82 > 1.27 for cladding and infill cases, respectively) indicating that cladding performs better than brick or adobe infill. The superior performance may be attributed to lower mass and better diaphragm action with nails connecting to the bare frame.
- The suspended weight on the tested frames was calculated assuming that there was a second floor and a light roof; however, the structural response may be favourably affected if the vertical load coming from upper floors were higher. During testing, one side of the frame goes into tension and failure is reached when the nails are driven off the base beam. Although additional upper floor(s) would cause more inertial lateral force to act on the base frame and P-Δ effects may worsen the response at large deformations, additional vertical load may be favourable for the member connections in tension.
- The *hımış* frames may be categorized as having "Medium capacity to dissipate energy—DCM" based on EC 8. The damage pattern of the frame tests clearly showed that the main energy dissipation mechanism is governed by the nailed connections. Therefore, making these connections more rigid may result in inferior energy dissipation properties at the connections and more brittle structural behaviour if timber members fail. Energy dissipation characteristics of the nailed connections seem to be characterizing the overall ductile response and energy dissipation properties of the tested *hımış* frames.
- The average capacity to demand ratio for bare frames in the nonlinear range is reduced from 1.33 to 1.27 in the case of infill while increased to 1.82 for cladding indicating that cladding is superior to infill. This result has significant importance for restoration and preservation studies for *hımış* houses, which have damaged infills and will go through major repair work. Cladding should be preferred to infill replacement whenever possible.
- Results showed that *hımış* houses with infill or cladding can survive a design earthquake with a certain amount of damage (without complete collapse), provided that the masonry ground floor (and other masonry sections of the building, if any) is strong enough to bear seismic loading and the timber skeleton is well connected to the

masonry ground floor. It should also be born in mind that the results reported here are valid for specific assumptions that have been explained in depth in relevant sections. Furthermore, it should also be considered that the tests and analyses reported here do not take the material degradation of existing *hımış* buildings into consideration as the frames tested here were of new timber. The conclusions drawn here therefore relate more to a certain building technology and typology, rather than to the existing building stock. Further research is necessary to investigate the impact of degradation on the capacity of *hımış* frames.

- The results should be evaluated bearing in mind that the workmanship has a very significant impact on the overall behaviour of the frames and the quality of the workmanship may vary considerably.
- ATC-40 should provide a robust assessment as it has been validated against other methods. FEMA 440 (2005) Chapter 10 gives a comparison of the current nonlinear static procedures given in FEMA 356 and ATC-40 and concludes for structures with behaviour type B that ATC-40 can result in "small underestimations or small overestimations of lateral displacement of systems with periods longer than about 0.6 s". As this is not the case for the frame set under examination here (Table 2), the drawn conclusions regarding the displacement response can be considered sufficiently robust. On the other hand, certain limitations of ATC-40 with regards to how to reflect the degrading stiffness and strength have been addressed in the following improvements. Similar research can be conducted using more recent ATC-55, ASCE 41-06 and ATC-58 to draw further conclusions about the seismic performance of the *hımış* frames and efficiency of each method. However, the essentials of the capacity spectrum method should remain substantially unchanged in all these documents.

Acknowledgments The authors are grateful to TÜBİTAK (The Scientific and Technological Research Council of Turkey) for providing financial assistance to conduct this research (No. 106M499) and to Profs Uğurhan Akyüz and Neriman Şahin Güçhan, and Dr Barış Erdil, and for their essential contributions in the frame tests. The authors would also like to thank Prof Dina D'Ayala for her invaluable feedback.

References

Aktaş YD, Akyüz U, Türer A, Erdil B, Şahin Güçhan N (2014a) Seismic resistance evaluation of traditional ottoman timber-frame Hımış houses: frame loadings and material tests. Earthq Spectra 30(4):1711–1732

Aktaş YD, Türer A, Akyüz U (2014b) Seismic performance assessment of traditional timber Hımış Frames by Laboratory Testing and Capacity Spectrum Method. In: 2nd European conference on earthquake engineering and seismology. Istanbul, Turkey, pp 28–38

Ambraseys NN, Zatopek A, Tasdemiroglu M, Aytun A (1968) The Mudurnu Valley (West Anatolia) Earthquake of 22 July 1967. UNESCO, Paris. Serial no. 622/BMS.RD/AVS

ATC (1996) Seismic evaluation and retrofit of concrete buildings ATC-40. Applied Technology Council (ATC), Redwood City, CA

Cerasi M (1998) The formation of ottoman house types: a comparative study in interaction with neighbouring cultures. Muqarnas 15:116–156

Demirtaş R, Iravul Y, Erkmen C, Baran B, Yaman M, Baykal M (2000) 06 Haziran 2000 Orta (Çankırı) Depremi. Jeoloji Mühendisleri Odası Haber Bülteni 1–2:6–15

Erdik M, Yuzugullu O, Yilmaz C, Akkas N (1992) 13 March, 1992 (Ms-6-8) Erzincan earthquake: a preliminary reconnaissance report. Soil Dyn Earthq Eng 11:279–310

Erdik M, Sesetyan K, Demircioglu MB, Celep U, Biro Y, Uckan E (2002a) Sultandağı earthquake, Turkey. Retrieved November 23, 2015, from Earthquake Engineering Research Institute, Learning From Earthquakes, Turkey. http://eeri.org/lfe/pdf/turkey_sultandagi_report_erdik.pdf

Erdik M, Sesetyan K, Demircioglu MB, Celep U, Biro Y, Uckan E (2002b). Special earthquake report from the May 2002 newsletter: preliminary observations on the Sultandağı, Turkey, Earthquake of February 3, 2002. Retrieved January 14, 2011. Retrieved November 23, 2015, from Earthquake Engineering Research Institute, Learning From Earthquakes, Turkey. http://www.eeri.org/lfe/pdf/Turkey_Sultandagi_Insert_May02.pdf

Erdik M, Demircioglu M, Beyen K, Sesetyan K, Aydinoglu N, Gul M et al (2003) May 01, 2003 Bingol (Turkey) earthquake. EERI. https://www.eeri.org/lfe/pdf/turkey_bingol_reconnaissance_report_erdik.pdf

European Committee for Standardization (2004) Design of structures for earthquake resistance part 1: general rules, seismic actions and rules for buildings. CEN, Brussels

FEMA (2005) FEMA 440: improvement of nonlinear static seismic analysis procedures. FEMA, California

Freeman SA (1998) The capacity spectrum method as a tool for seismic design. In: 11th European conference on earthquake engineering. Balkema, Paris

Gülhan D, Özyörük Güney İ (2000) The behaviour of traditional building systems against earthquake and its comparison to reinforced concrete frame systems: experiences of Marmara earthquake damage assessment studies in Kocaeli and Sakarya. In: Earthquake-safe: lessons to be learned from traditional buildings. ICOMOS, Istanbul

Hayashi Y, Nii A, Morii T (2008) Evaluation of building damage based on equivalent-performance response spectra. In: 14th world conference on earthquake engineering. Beijing

Kawai N (1999) Prediction methods for earthquake response of shear walls. In: Pacific timber engineering conference. Rotorua, pp 317–324

Kawai N (2000) Application of capacity spectrum method to timber houses considering shear deformation in horizontal frames. In: World conference on timber engineering. Whistler, BC

Koçyiğit A, Bozkurt E, Kaymakcı N, Şaroğlu F (2002) 3 Şubat 2002 Çay (Afyon) Depreminin Kaynağı ve Ağır Hasarın Nedenleri: Akşehir Fay Zonu (Jeolojik Ön Rapor). Retrieved December 08, 2013. http://www.metu.edu.tr/~akoc/Afyon.pdf

Kuban D (1995) The Turkish Hayat house. T.C. Ziraat Bankası Kültür Yayınları, Istanbul

Langenbach R (2007) From “Opus Craticium” to the “Chicago Frame”: earthquake-resistant traditional construction. Int J Archit Herit 1:29–59

Penzien J, Hanson RD (1970) The Gediz, Turkey, earthquake of 1970: a report to the national science. National Academy of Sciences for the National Academy of Engineering, Washington

Şahin Güçhan N (2007) Observations on earthquake resistance of traditional timber framed houses in Turkey. Build Environ 42:840–851

Sözen M (2001) Türklerde Ev Kültürü. Doğan Kitapçılık A.Ş, Istanbul

Tobriner S (2000) Wooden architecture and earthquakes in Turkey: a renaissance report and commentary on the performance of wooden structures in the Turkish earthquakes of 17 August and 12 November 1999. In: Earthquake-safe: lessons to be learned from traditional buildings. ICOMOS, Istanbul